A Two-Dimensional Transmission Line Matrix Microwave Field Simulator Using New Concepts and Procedures

POMAN P. M. SO, MEMBER, IEEE, ESWARAPPA, STUDENT MEMBER, IEEE, AND WOLFGANG J. R. HOEFER, SENIOR MEMBER, IEEE

Abstract—**A two-dimensional field simulator for microwave circuit modeling is described. It incorporates a number of novel concepts and advanced transmission line matrix (TLM) procedures recently developed at the University of Ottawa. In particular, a discrete Green's function concept based on Johns's time-domain diakoptics has been realized, providing unprecedented processing power through modularization of large structures at the field level, simulation of wide-band matched loads or absorbing walls, modeling of frequency-dispersive boundaries in the time domain, and large-scale numerical preprocessing of passive structures. Nonlinear field modeling concepts have also been implemented in the TLM field simulator. It can analyze two-dimensional circuits of arbitrary geometry containing both linear and nonlinear media. The circuit topology is input graphically. Both time-domain and frequency-domain responses can be computed and displayed. The capabilities and limitations of the simulator are discussed, and several microstrip and waveguide components are modeled to demonstrate its important features.**

I. Introduction

THE TRANSMISSION line matrix (TLM) method was invented and pioneered by Johns and Beurle [1]. Extensive lists of references on this subject can be found in two review papers [2] and [3] and in a book chapter on TLM [4] by Hoefer. The powerful and versatile TLM algorithm is suitable for microwave and millimeter-wave circuit simulation, especially when the circuit geometry is highly irregular. The most tedious and error-prone part of a TLM simulation is usually the preparation of an input file which specifies the geometry, dielectric properties, excitation and output features. We have therefore developed a two-dimensional TLM field simulator which incorporates software for defining the layout of the circuit graphically on the screen, locating the input and output points, and specifying the desired excitation function in analytical or digital form. The simulator can be used in two different ways: It can compute and display the time-domain response of a circuit to an arbitrary waveform, or it can compute the impulse response of a circuit and extract its complex S parameters (magnitude and phase) in the frequency domain via Fourier transform. In all cases, the spectrum of input and output signals can be displayed. Both linear and nonlinear field analyses can be performed, and transient as well as steady-state behavior can be studied directly on the screen.

To realize these capabilities, a number of advanced TLM procedures have been developed, including a wide-band absorbing boundary condition for non-TEM simulation using a numerical Green's function derived from Johns's time-domain diakoptics [5], matched impulsive voltage sources, a numerical procedure for the separation of incident and reflected fields in S-parameter computations, and nonlinear TLM nodes.

In this paper, these features will be described, and some typical simulation results will be presented to demonstrate the versatility and accuracy of the TLM field simulator. A three-dimensional simulator is presently being developed which employs the same advanced procedures for parameter extraction as the two-dimensional version but overcomes the limitations of two-dimensional modeling.

II. Linear and Nonlinear TLM Field Modeling

A. Linear Field Modeling

The TLM method is a numerical modeling tool for electromagnetic fields in space and time. Unlike other time-domain methods, which are based on the discretization of Maxwell's or Helmholtz's time-dependent equations, the TLM method embodies Huygens's principle in discretized form. In a typical TLM simulation, the field space is filled with a dense mesh of transmission lines. Boundaries are modeled by appropriate reflection coefficients. The mesh is then excited by one or several voltage impulses which spread throughout the structure and are scattered at the nodes and boundaries. The analysis of this process is conveniently described in terms of incident and reflected impulses, V^i and V^r, on the transmission lines at the nodes of the network. The algorithm can be formulated as an iterative sequence of the following operations:

$$[V]^r_{k+1} = [S]\cdot[V]^i_k \tag{1}$$

$$[V]^i_{k+1} = [C]\cdot[V]^r_{k+1} \tag{2}$$

Manuscript received March 4, 1989; revised July 5, 1989. This work was supported by the Natural Science and Engineering Research Council of Canada and by the Government of Ontario through the Telecommunications Research Institute of Ontario (TRIO).

The authors are with the Laboratory for Electromagnetics and Microwaves, Department of Electrical Engineering, University of Ottawa, Ottawa, Canada K1N 6N5.

IEEE Log Number 8930816.

where $[S]$ is the impulse scattering matrix of the nodes, and $[C]$ is a connection matrix describing the topology of the network. The subscripts k and $k+1$ denote the discrete time intervals at which the incident and the reflected impulses in the branches of each node are computed. Scattering events are separated in time by Δt during which an impulse travels across the mesh parameter Δl at the speed of light.

Frequency-domain characteristics can be extracted from the impulse response of the mesh via discrete or fast Fourier transform. One single TLM analysis thus yields complete information on S parameters, dispersion characteristics, and field configuration over a wide frequency range.

B. Modeling of Frequency Dispersive Boundaries in the Time Domain

Modeling perfect electric and magnetic walls is straightforward in a TLM simulation: the impulses incident upon such boundaries are simply reflected with the appropriate real reflection coefficient. However, frequency dispersive boundaries, such as wide-band absorbing walls in non-TEM waveguides, lead to complex or dispersive reflection coefficients. Dirac impulses incident upon such walls are broadened and distorted. The TLM method cannot account for this effect since it is a discretized procedure.

Two possible solutions to this problem can be implemented.

The first solution is to approximate the dispersive reflection coefficient by a nondispersive one. This gives accurate results only at a single frequency for which the approximation is valid. Such a narrow-band solution does not fully exploit the wide-band capability of the TLM approach, but is easily implemented, requiring no additional processing.

The second solution—implemented for the first time in this simulator—is to represent the dispersive boundary by a characteristic impulse response or numerical Green's function. A single impulse incident upon the boundary causes not just one reflected impulse, but a whole stream of impulses. To visualize this concept, consider the short-circuited waveguide section in Fig. 1. The stub of width a and length l, within the operating range of the dominant TE_{10} mode, has a frequency dispersive input reflection coefficient Γ_{in},

$$\Gamma_{in} = -e^{-2j\beta l} \tag{3}$$

where β is the phase constant of the TE_{10} mode. To represent this reflection coefficient in the time domain, we model the waveguide stub by a two-dimensional shunt mesh as shown in Fig. 1. Note that all boundaries are placed halfway between nodes to ensure synchronism of impulses throughout the TLM mesh. The branches penetrating through the input plane (also called removed branches) are numbered 1 through $M = N$. An impulse entering any one of these branches, let us say branch 1, will result in a stream of impulses emerging from all M branches. These impulse functions result from the scattering at the nodes and boundaries of the structure, and can be interpreted as a Green's function in numerical form. All removed branches are terminated in their own characteristic impedance during this procedure so as to absorb the emerging output streams.

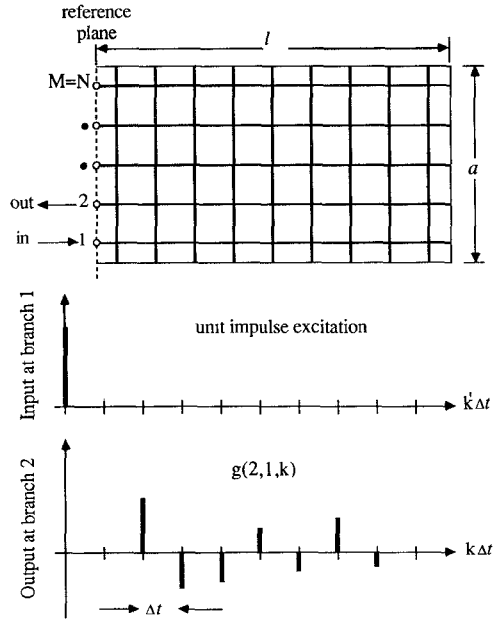

Fig. 1. 2-D TLM mesh modeling a short-circuit waveguide stub. The reference plane is a frequency dispersive impedance wall. One term of its time signature, or Johns matrix, $g(2,1,k)$, is shown.

Fig. 1 shows, as an example, the impulse output function at branch 2 resulting from a single unit impulse entering branch 1 at $t' = k'\Delta t = 0$. In general terms, if we call $g(m, n, k)$ the output impulse function emerging at the mth branch due to a unit excitation of the nth branch at $t = k\Delta t$, the complete numerical Green's function for the input plane of the waveguide stub can be written in matrix form as follows:

$$\begin{matrix} g(1,1,K) & \cdots & g(1,n,K) & \cdots & g(1,N,K) \\ g(1,1,k) & \cdots & g(1,n,k) & \cdots & g(1,N,k) \\ g(1,1,0) & \cdots & g(1,n,0) & \cdots & g(1,N,0) \\ & & & & g(m,N,K) \\ & & & & g(m,N,k) \\ g(m,1,0) & \cdots & g(m,n,0) & \cdots & g(m,N,0) \\ & & & & g(M,N,K) \\ & & & & g(M,N,k) \\ g(M,1,0) & \cdots & g(M,n,0) & \cdots & g(M,N,0) \end{matrix} \tag{4}$$

(m: row index; n: column index; k: time index)

Here $N = M$ is the total number of removed branches in the reference plane, and K is the total number of iterations. We propose the term *Johns matrix* for this characteristic function in honour of the late P. B. Johns, pioneer of TLM and time-domain diakoptics.

The general problem to be solved is the computation of the component's time response to arbitrary streams of impulses entering its input branches. The input or excitation function is the column vector of voltage impulse streams $[V^i(n,k')]$ incident on all branches 1 to N, while the output function would be the resulting $[V^r(m,k)]$

emerging from the branches 1 to M. The latter is obtained by a restricted convolution of the Johns matrix with the input excitation function [5]:

$$[V^r(m,k)] = [G(m,n,k')] * [V^i(n,k')]. \quad (5)$$

The kth time sample of the output impulse function at the mth branch is computed as follows:

$$v^r(m,k) = \sum_{n=1}^{N} \sum_{k'=0}^{k} g(m,n,k') v^i(n,k-k'). \quad (6)$$

This convolution algorithm has been implemented in the TLM field simulator to model wide-band absorbing boundaries for non-TEM simulations.

Obviously, this convolution process represents an extension of the scattering parameter concept into the time dimension. It opens unprecedented possibilities for partitioning of time-domain field problems and permits large-scale numerical preprocessing of electromagnetic substructures for CAD.

C. Nonlinear Field Modeling

Nonlinear and time-dependent field parameters can be modeled by updating the properties of the TLM mesh at each iteration. For example, the characteristic admittances of permittivity and loss stubs determine the dielectric constant and the conductivity of a medium through the impulse scattering matrix $[S]$ of the nodes to which they are attached. Since voltage and current are computed at all nodes for each iteration, the stub admittances can be recalculated and updated accordingly to simulate nonlinear behavior. Similarly, the energy absorbed during a simulation can be translated into a temperature change resulting in a change in ϵ and σ. The small time delay Δt between cause and effect in the model is usually negligible vis-à-vis the period of the highest frequency component of the fields.

In this paper, the nonlinear capability of the TLM field simulator is used to model a varactor frequency multiplier in combination with a calibrated voltage impulse source. The various features of the simulator are based on these concepts and will be described below.

III. Implementation of Field Simulation Modules

A. Implementation of Absorbing Boundaries

Absorbing boundaries are among the most important features in field modeling. They play the same role as the anechoic chamber in antenna work or the matched load in transmission line and waveguide measurements. One can distinguish between absorbing boundaries for TEM and for non-TEM waves. The former can usually be represented by a nondispersive impedance, while the latter have a frequency-dependent impedance.

1) TEM Absorbing Boundaries: In two-dimensional plane wave TLM simulation, such as parallel-plate modeling of microstrip, a wide-band absorbing load for the TEM mode is modeled by terminating the individual mesh lines

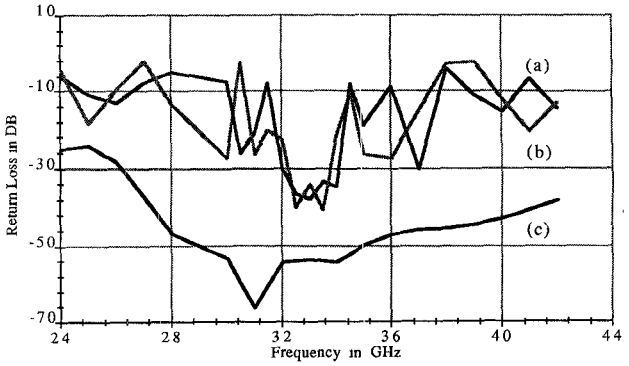

Fig. 2. A comparison of the return loss characteristics of absorbing waveguide boundaries obtained by two different methods. (a) Termination with $Z_w/\sqrt{2}$ and 1500 iterations. (b) Termination with $Z_w/\sqrt{2}$ and 2500 iterations. (c) Termination with the Johns matrix.

(impedance Z_0) with the intrinsic impedance of the TLM mesh, $Z_0/\sqrt{2\epsilon_{\text{eff}}}$, where ϵ_{eff} is the effective relative permittivity of the microstrip line. Note that this results in a nonzero reflection coefficient for the individual impulses traveling on the mesh lines toward the boundary, while the total energy moving in the form of a traveling "mass action" wave is completely absorbed by it. This is consistent with Huygens's principle, which stipulates that each point of a moving wavefront emits secondary wavelets in all directions, including the backward one.

2) Narrow-band Non-TEM Absorbing Boundaries: In non-TEM wave simulations, such as waveguide modeling, the mesh lines must be terminated with a dispersive wave impedance $Z_0/\sqrt{2\left(\epsilon_r - (f_c/f)^2\right)}$, where ϵ_r is the relative permittivity of the medium filling the guide and f_c is the cutoff frequency. This poses no problem in frequency-domain analysis. However, when a waveguide component is analyzed by impulsive excitation followed by Fourier transform, termination in a single impedance gives accurate results only for the frequency at which that impedance represents a match, as mentioned in the introduction. At best, this approach leads to a narrow-band absorbing condition, which is acceptable when the frequency range of interest is only a fraction of an octave. The frequency behavior of such a termination is shown in Fig. 2.

3) Generalized Wide-band Absorbing Boundaries: To model truly wide-band absorbing boundaries over a large frequency range and for all field types, the discrete Green's function, or Johns matrix approach described in subsection II-B must be implemented. In other words, we must simulate and store the response to unit excitations of a wide-band absorbing boundary, and then convolve its Johns matrix with the impulses incident upon it during subsequent TLM runs. For the purpose of modeling wide-band matched waveguide loads with the two-dimensional field simulator, we have employed two different approaches:

a) We have modeled a waveguide termination containing a lossy medium with gradually increasing loss tangent. The length and loss profile of this termination depend upon the bandwidth over which reflec-

tions are to be kept small. To simulate good absorbing conditions over the operating band of a standard rectangular waveguide, a length of about $4\lambda_g$ at midband frequency is required. Touchstone™ CAD software has been used to optimize the loss profile of the termination.

b) We have modeled a waveguide section so long that reflections from the far end cannot return to the input reference plane before the computation is stopped. Thus, a section of $1000\Delta l$ yields a Johns matrix with up to 2000 time samples.

Both these approaches yield almost identical results of excellent quality. In Fig. 2 the performances of a narrow-band and a wide-band waveguide termination are compared. To obtain these characteristics, a uniform section of WR28 waveguide, $50\Delta l$ long, was terminated at both ends with simulated absorbing walls. After impulsive excitation followed by several thousand iterations, the standing wave ratio in the waveguide section was determined between 24 and 44 GHz by Fourier transform of the impulse response of the system. The cascaded return loss of the opposing absorbing boundaries, obtained as $20\log[(VSWR-1)/(VSWR+1)]$, is shown in Fig. 2 over a frequency range exceeding the recommended operating range of the guide, 26.5–40 GHz.

The narrow-band absorbing walls were modeled by terminating the mesh lines at the boundary positions with $Z_w/\sqrt{2}$, where Z_w is the wave impedance at the midband frequency of 33 GHz. Results are shown for two different numbers of iterations. Reflections are small only between 32 and 34 GHz and depend on the number of iterations. Since the Fourier transform of the time-domain results is very sensitive to imperfect absorbing boundary conditions, the accurate computation of S parameters is not possible over a wide band of frequencies with this termination.

The wide-band absorbing walls were modeled by the Johns matrix obtained as described in a) above. The superior performance of this model is immediately obvious. We conclude that a single such boundary has a return loss of better than -35dB across the operating range of the guide.

The Johns matrix is a three-dimensional array $G(M,N,K)$ of size $M \times N \times K$, where $M = N$ is the number of mesh lines entering the simulated boundary, and K is the total number of iterations. The Johns matrix has, however, been reduced to a one-dimensional array $G(K)$ by assuming that the waveguide field is that of a propagating mode with known field distribution. This implies that the absorbing termination is placed beyond the reach of higher order modes, i.e., about a quarter wavelength away from the nearest discontinuity. The resulting savings in memory storage for the Johns matrix and in convolution time (reduction by a factor $M \times N$ for both) are considerable. This modal Johns matrix procedure to simulate the above wide-band waveguide match takes about one order of magnitude less time and memory than the full discretization and simulation of a lossy termination.

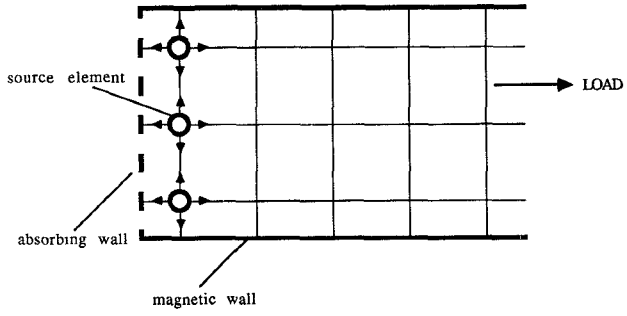

Fig. 3. Simulation of a matched voltage source in a parallel-plate waveguide with magnetic sidewalls.

B. Modeling of Calibrated Impulse Voltage Sources

For nonlinear field modeling it is necessary to have sources which generate fields of known absolute amplitude at any frequency. They can be realized in the form of Huygens sources backed by an absorbing wall on the side opposite to the load (see Fig. 3). The magnitude of the voltage impulses, V_k^s, launched from each source into its four main branches must be $\sqrt{2\epsilon_{\text{eff}}}$ times the field amplitude, V_{mesh}^+, of the desired traveling wave at the corresponding transversal position in the mesh:

$$V_k^s = \sqrt{2\epsilon_{\text{eff}}} \times V_{\text{mesh}}^+. \tag{7}$$

If the structure is a TEM waveguide (as in Fig. 3) all sources have the same weight, and ϵ_{eff} is the dielectric constant in the TEM structure. If the structure is a rectangular waveguide carrying the TE_{10} mode, the weight of the sources is distributed in a sinusoidal fashion, and ϵ_{eff} is obtained as

$$\epsilon_{\text{eff}} = \epsilon_r - \left(\frac{\lambda}{\lambda_c}\right)^2 \tag{8}$$

where ϵ_r is the dielectric constant filling the waveguide, and λ and λ_c are the free-space and cutoff wavelengths, respectively.

It is easily observed that a complicated waveform injected into a non-TEM waveguide will be distorted due to the frequency dispersive nature of the effective waveguide permittivity. However, for the most practical case of single-frequency excitation, the traveling wave amplitude can be set using (7) and (8).

C. Extraction of S Parameters from the TLM Impulse Response

The scattering parameters of n-ports are computed by injecting an impulse wave into one of the ports, computing the impulse response in all ports when they are terminated in a wide-band absorbing load, and taking their Fourier transform. Since S parameters are relative quantities, the Fourier transform of the transmitted voltages, $\bar{V}_{\text{trans}}$, must be divided by that of the incident voltage, $\bar{V}_{\text{inc}}$. The latter can easily be computed by modeling the input section of the structure (source and input guide up to the input

reference plane), replacing the n-port by a wide-band absorbing boundary. The input reflection coefficient of the n-port is obtained by computing the complex reflected voltage, $\overline{V}_{\text{refl}}$, at the input plane as

$$\overline{V}_{\text{refl}} = \frac{\overline{V}_{\text{tot}} - \overline{V}_{\text{inc}}}{\overline{V}_{\text{inc}}} \tag{9}$$

where $\overline{V}_{\text{tot}}$ is the Fourier transformed impulse response of the device in the input arm.

Thus, by capitalizing on our ability to model good wide-band absorbing boundaries, we have greatly improved the S-parameter extraction procedure. In the past, S_{11} has been computed by finding the amplitudes and positions of voltage maxima and minima in the input port, as in a slotted line measurement. This required an input line at least several wavelengths long, and a very fine discretization was needed to compute the magnitude and phase of S_{11} accurately.

The propagation constant of the input waveguide section is also obtained from the incident field function $\overline{V}_{\text{inc}}$.

IV. Simulation Examples

The following simulation examples demonstrate the implementation and performance of these new concepts and procedures. We have modeled a microstrip lowpass filter, a microstrip varactor multiplier, and an iris-coupled waveguide bandpass filter, and compared the results with other methods.

A. Modeling of a Microstrip Low-Pass Filter

In commercial CAD software, microstrip lines and discontinuities are modeled by empirical expressions for their effective permittivity and characteristic impedance. These expressions are quite accurate and take frequency dispersion of the quasi-TEM mode into account.

To model such circuits in the time domain with our two-dimensional field simulator, we must first define a parallel-plate equivalent model with nondispersive effective permittivity. It has been shown by Menzel and Wolff [6] that such an approximation gives quite good results at relatively low frequencies, even for discontinuities such as impedance steps and T junctions. This parallel-plate model can then be discretized and analyzed with the TLM method.

The effective width of that model for a straight microstrip line section can be computed using the formulas given by Hammerstad and Jensen [7] or similar formulas. The effective dielectric constant of the line is simulated by permittivity stubs attached to the TLM nodes inside the model. The normalized characteristic admittance of the stubs is $y_0 = 4(\epsilon_{\text{eff}} - 1)$.

Fig. 4 shows the topology of the parallel-plate model of a microstrip low-pass filter discretized for TLM simulation, as defined on the screen of the simulator. A unit matched impulse source is implemented at the left extremity, and an absorbing wall terminates the output port. Fig. 5 compares the magnitude and phase of the S parameters of the low-pass filter as obtained with the simulator and

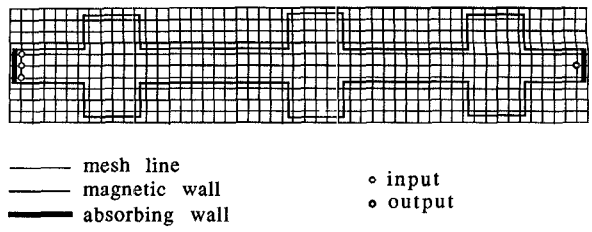

Fig. 4. The equivalent 2-D TLM model (loading stubs are not shown) of a microstrip low-pass filter ($\epsilon_r = 9.60$, $\epsilon_{\text{eff}} = 8.22$, $\Delta l = 1$ mm).

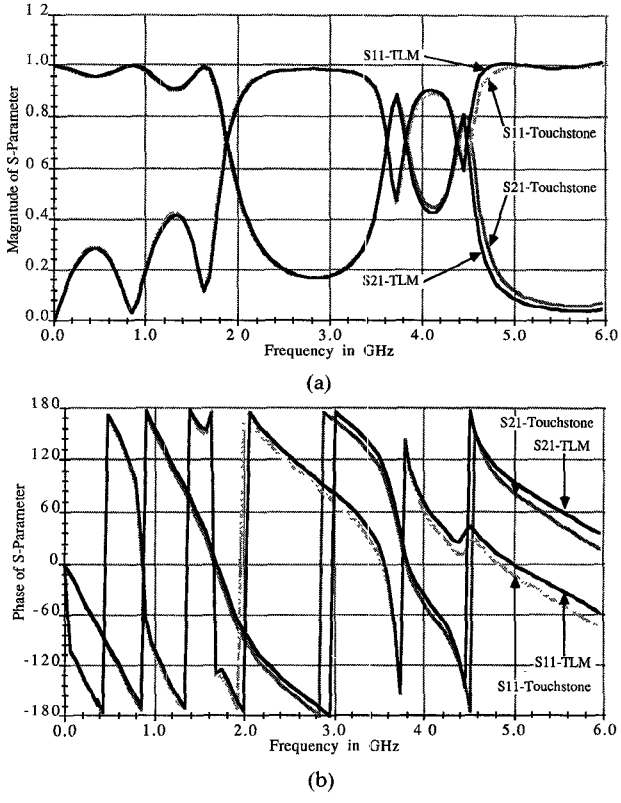

Fig. 5. A comparison of microstrip low-pass filter characteristics obtained by using Touchstone and the TLM method. (a) Magnitude of S_{21} and S_{11}. (b) Phase of S_{21} and S_{11}.

with Touchstone. Note the excellent agreement up to about 4 GHz. At higher frequencies, dispersion effects, which are included in Touchstone but not in the 2-D TLM model, lead to disagreement. Only a three-dimensional TLM analysis can properly model the dispersive microstrip behavior.

B. Modeling of a Microstrip Varactor Multiplier

To demonstrate the capability of TLM to model nonlinear problems, we have simulated a simple frequency multiplier featuring a varactor diode in a parallel-plate waveguide (microstrip model).

The diode is represented by a voltage-dependent capacity which, in turn, appears as a subsection of the microstrip model with a voltage-dependent permittivity such that the capacity of the subsection is equal to that of the varactor. The area of the nonlinear subsection is the same as that of a real packaged diode, and it is considered small compared with the shortest wavelength of interest in the

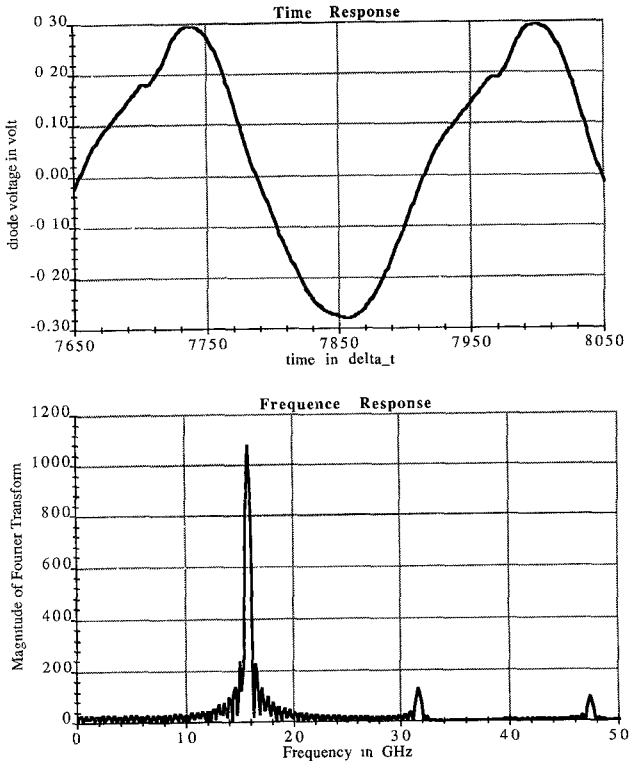

Fig. 6. The output waveform of a varactor multiplier and its output spectrum, simulated by TLM, at $V_{\text{bias}} = 0.2$ V and V^{+}_{mesh} having an amplitude of 1 V.

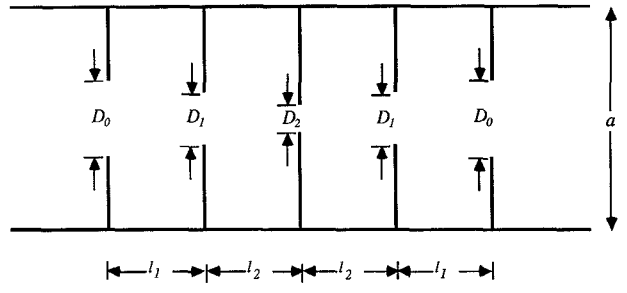

Fig. 7. The geometry of a four-section Chebyshev iris-coupled bandpass filter.

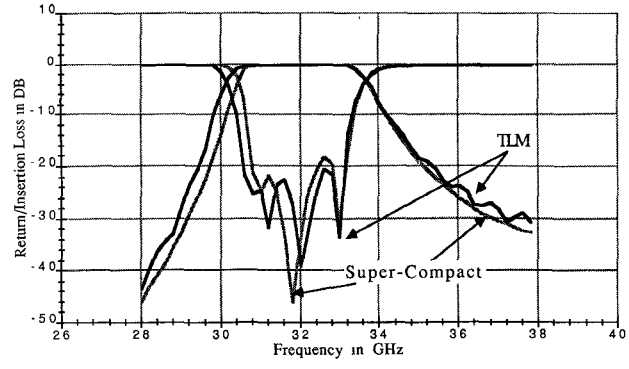

Fig. 8. A comparison of the return loss and insertion loss characteristics, obtained by the lumped element model and the TLM method, of a waveguide-iris-coupled bandpass filter.

simulation. Nonlinear behavior is modeled by updating at each iteration the characteristic stub admittance y_0 in the subsection as a function of the instantaneous voltage at a node in the center of the subsection [8]. It is given by

$$y_0 = 4\left[\frac{C_{jv} + C_{dv} + C_p}{C_a} - 1\right] \tag{10}$$

where

C_{jv} = voltage-dependent junction capacitance

$$= \frac{C_{jb}}{\sqrt{1 - \dfrac{v(t)}{\phi_0 - V_{\text{bias}}}}}$$

$$C_{jb} = \frac{C_{j0}}{\sqrt{1 - \dfrac{V_{\text{bias}}}{\phi_0}}}$$

C_{j0} = zero bias capacitance of the diode,

C_{dv} = voltage-dependent diffusion capacitance of the diode

$= 3.212 \times 10^{-18} e^{40 \times v(t) + V_{\text{bias}}}$,

C_p = package capacitance,

C_a = capacitance of the diode subsection when filled with ϵ_{eff} of the microstrip,

ϕ_0 = built-in potential.

A sinusoidal voltage sampled at intervals of Δt was injected using a calibrated source, as shown in Fig. 3.

Fig. 6 shows the steady-state waveform at the output point and its Fourier transform (spectrum). The nonlinear effects and the generation of harmonics are clearly visible. This nonlinear 2-D TLM model has been used to design varactor frequency multipliers and dividers [8]. Measured results were in good agreement with the simulation results.

C. Modeling of an Iris-Coupled Rectangular Waveguide Bandpass Filter

To simulate the reflection and transmission characteristics of waveguide components, wide-band absorbing loads must be implemented using the Johns matrix approach. Fig. 7 shows the geometry of a four-section Chebyshev iris-coupled waveguide bandpass filter with the following characteristics:

center frequency = 32 GHz
bandwidth = 2 GHz
passband ripple = 0.01 dB (equivalent to 26dB return loss)
guide width = 7.112 mm.

The dimensions of the filter were calculated following the design method given in [9]. They are

$D_0 = 3.580$ mm
$D_1 = 2.340$ mm
$D_2 = 2.050$ mm
$l_1 = 4.954$ mm
$l_2 = 5.591$ mm.

The return loss and transmission loss computed with the Johns matrix approach are given in Fig. 8. For comparison, this bandpass filter was analyzed with Super-Compact™, accounting for the frequency-dependent susceptance of the irises [10]. The results obtained with the two methods are compared in Fig. 8. They agree well.

V. Conclusion

A user-friendly two-dimensional field simulator based on the TLM method has been described. It allows the user to enter the circuit topology and its dielectric characteristics directly on the screen and to observe both the time and frequency responses of the circuit as the simulation progresses in time. Complex S parameters for a wide frequency band can be extracted from a single impulse response computation. Both linear and nonlinear simulations can be performed, and the time response of a structure to an arbitrary excitation function can be modeled and displayed.

To achieve these capabilities, a number of innovative concepts have been developed and implemented. The most important of them is the representation in the time domain of frequency dispersive boundaries by a discrete characteristic time signature, or Johns matrix, which is analogous to the Green's function concept in classical electromagnetic theory. This concept has been implemented to model wide-band matched terminations in waveguides and to partition large structures into smaller substructures using time-domain diakoptics. Other new features, such as matched calibrated voltage sources, nonlinear TLM nodes, and an S-parameter extraction algorithm, have also been included in the simulator.

The present limitation to two dimensions restricts the usefulness of the simulator for microstrip and waveguide modeling. However, any truly two-dimensional problem of arbitrary geometry can be modeled effectively and with a great level of confidence, as the above examples indicate. The errors inherent in TLM modeling are determined essentially by the TLM mesh size, which in turn is limited by the memory and speed of the computer used. The algorithm itself is unconditionally stable and is guaranteed to converge. The convolution process in the Johns matrix approach does not introduce any significant deviation from traditional TLM modeling results (less than 10^{-5}).

The importance of this simulator resides in the demonstration and implementation of new concepts which open unprecedented possibilities for efficient time-domain modeling of large and complicated structures. We are now working on a three-dimensional field simulator which will incorporate these advanced features, for the modeling of MMIC and EMI/EMC problems.

References

[1] P. B. Johns and R. L. Beurle, "Numerical solution of 2-dimensional scattering problems using a transmission-line matrix," *Proc. Inst. Elec. Eng.*, vol. 118, no. 9, pp. 1203–1208, Sept. 1971.

[2] W. J. R. Hoefer, "The transmission-line matrix method—Theory and applications," *IEEE Trans. Microwave Theory Tech.*, vol. MTT-33, pp. 882–893, Oct. 1985.

[3] W. J. R. Hoefer, "Linear and nonlinear field modeling in the time domain with the transmission line matrix (TLM) method," *Alta Frequenza*, vol. LVIII, Aug. 1989.

[4] W. J. R. Hoefer, "The transmission line matrix (TLM) method," in *Numerical Techniques for Microwave and Millimeter Wave Passive Structures*, T. Itoh, Ed. New York: Wiley, 1989.

[5] P. B. Johns and K. Akhtarzad, "The use of time domain diakoptics in discrete models of fields," *Int. J. Numer. Meth. Eng.*, vol. 17, no. 14, pp. 1–14, 1981.

[6] W. Menzel and I. Wolff, "A method for calculating the frequency-dependent properties of microstrip discontinuities," *IEEE Trans. Microwave Theory Tech.*, vol. MTT-25, pp. 107–112, Feb. 1977.

[7] E. O. Hammerstad and O. Jensen, "Accurate models for microstrip computer aided design," in *IEEE MTT-S Int. Microwave Symp. Dig.*, 1980, pp. 407–409.

[8] S. A. Kosmopoulos, W. J. R. Hoefer, and A. Gagnon, " Non-linear TLM modeling of high-frequency varactor multipliers and halvers," in *Proc. 13th Int. Conf. Infrared and Millimeter Waves*, (Hawaii), Dec. 1988, pp. 239–240.

[9] G. Matthaei, L. Young, and E. M. T. Jones, *Microwave Filters, Impedance-Matching Networks and Coupling Structures*. New York: McGraw-Hill, 1964.

[10] N. Marcuvitz, *Waveguide Handbook*. New York: Dover, 1965.

Poman P. M. So (S'86–M'88) was born in Hong Kong on March 15, 1961. He received the B.S.c. degree in computer science and physics from the University of Toronto, Toronto, Ontario, Canada, in 1985. He obtained the B.A.Sc. degree in electrical engineering (summa cum laude) from the University of Ottawa, Ottawa, Ontario, Canada, in 1987. He has been engaged in research on the computer-aided design of microwave and millimeter-wave circuits, TLM techniques for solving electromagnetic problems. Mr. So is currently working toward the M.A.Sc. degree in Electrical Engineering at the University of Ottawa. Since January 1989, he has been a research engineer in the University of Ottawa.

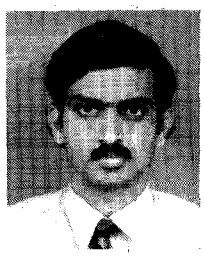

Eswarappa (S'89) received the B.E. degree in electronics and communication from Mysore University, India, in 1980 and the M.Tech degree in electrical engineering from the Indian Institute of Technology, Kanpur, in 1982.

From 1982 to 1986, he worked as an Assistant Executive Engineer in the Transmission Research and Development Laboratory, Indian Telephone Industries, Bangalore, India. He was mainly engaged in the design and development of microwave circuits and the characterization of microstrip discontinuities. Since 1986 he has been engaged in research on quasi-planar transmission media and numerical techniques, and he is working toward the Ph.D degree in electrical engineering at the University of Ottawa, Ottawa, Ont., Canada.

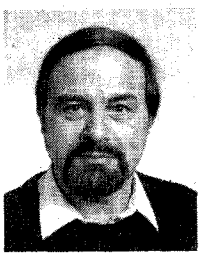

Wolfgang J. R. Hoefer (M'71–SM'78) received the diploma in electrical engineering from the Technische Hochschule Aachen, Aachen, Germany, in 1964 and the D. Ing. degree from the University of Grenoble, Grenoble, France, in 1968.

After one year of teaching and research at the Institut Universitaire de Technologie, Grenoble, France, he joined the Department of Electrical Engineering, University of Ottawa, Ottawa, Ont., Canada, where he is currently a Professor. His sabbatical activities have included six months with the Space Division of the AEG-Telefunken in Backnang, Germany, six months with the Electromagnetics Laboratory of the Institut National Polytechnique de Grenoble, France, and one year with the Space Electronics Directorate of the Communications Research Centre in Ottawa, Canada. His research interests include microwave measurement techniques, millimeter-wave circuit design, and numerical techniques for solving electromagnetic problems.

Dr. Hoefer is a registered Professional Engineer in the province of Ontario, Canada.